Diffraction from surface growth fronts

H.-N. Yang, T.-M. Lu, and G.-C. Wang
Department of Physics, Rensselaer Polytechnic Institute, Troy, New York 12180-3590
(Received 17 June 1992)

The characteristics of a multilayer stepped surface structure relevant to the growth of thin films has been described in the reciprocal space based on the dynamic scaling description of the interface growth. It is shown that the angular intensity distribution of a diffraction beam, in general, contains a δ function at the central peak position and a diffuse intensity which is a sum of an infinite number of special functions with different widths. At the vicinity of the in-phase diffraction condition, the δ intensity is the dominant component in the angular profile, which shows a steady decay as a function of the growth time. In contrast, at the near out-of-phase diffraction condition, the angular profiles become purely diffusive and time invariant. This time-invariant behavior reflects the dynamic scaling characteristics of thin-film growth. The applications of the theory to techniques such as x-ray diffraction, electron diffraction, and light scattering are discussed. It is shown that the growth exponents associated with the growth parameters such as the surface width can be easily obtained from the measured diffraction intensity using these diffraction techniques.

I. INTRODUCTION

Recently, there has been a dramatic increase of theoretical research activities in the area of surface growth dynamics.[1-3] Growth processes are inherently nonequilibrium processes. A systematic statistical approach to the nonequilibrium problem has not been developed thus far and therefore it cannot be used to describe the growth process. However, theorists recently have shown that a dynamic scaling approach is very fruitful in describing the growth dynamics. In dynamic scaling, the morphology of a growing interface is proposed to have a self-affine form. The interface width which describes the surface height fluctuation is scaled as[1-3]

$$w(L,t)\approx L^{\alpha} f\left[\frac{t}{L^{z}}\right], \tag{1a}$$

where $z=\alpha/\beta$ and L is the finite size of the system. The scaling function $f(x)$ is given by

$$f(x)\approx \begin{cases} x^{\beta} & \text{for } x \ll 1 \\ \text{const} & \text{for } x \gg 1. \end{cases} \tag{1b}$$

For $L^{z} \gg t$, the interface width grows with time in a form of power law, $w \sim t^{\beta}$, while for $L^{z} \ll t$, $w \sim L^{\alpha}$, showing that the interface morphology has a stationary self-affine form. The exponent β describes the growth rate of the interface width. The exponent α $(0 \leq \alpha \leq 1)$ is a measure of the surface roughness. Within the dynamical scaling approach, different growth models, such as the random growth model,[4-6] Eden model,[7-9] ballistic deposition,[10,11] Kardar, Parisi, and Zhang model,[12] and the restricted solid-on-solid model,[13] would give different values of the growth exponents. Recent studies also concentrated on the growth models which simulate molecular-beam-epitaxy (MBE) processes.[14-17]

Experiments designed to clarify issues in growth dynamics have been very scarce. There was an indirect approach reported recently in a crystalline interface etched by ion bombardments (instead of growth).[18] Static multilayer rough interfaces have been studied extensively. The most recent studies include the determination of the roughness correlations in multilayer films for x-ray mirrors[19] and the characterization of fractal properties of polycrystals, amorphous, or porous media.[20,21] However, experimental tests of recently developed dynamical models using technologically important growth techniques such as MBE and metal-organic chemical-vapor deposition have not been reported. A successful experiment requires a characterization technique (or techniques) to measure the relevant growth parameters during growth. Both direct imaging techniques (such as scanning tunneling microscopy and scanning electron microscopy) and diffraction techniques [such as low-energy electron diffraction (LEED) and x-ray diffraction] can be used for this purpose. We shall discuss only diffraction techniques.

Although kinematic diffraction theories from numerous model surfaces containing stepped structures have been developed in the past, rigorously speaking, most of them are not suitable for a description of scaling behavior in growth dynamics involving a large number of atomic layers. Diffraction from surfaces containing unrestricted numbers of atomic layers[22] and from surfaces undergoing roughening transitions[23,24] have a diverging surface width as the size of the surface becomes large. In the growth problem, the surface is normally assumed to contain a finite level of steps (except for the case where the growth takes place above the roughening transition temperature).

Diffraction theories for a small number of atomic lay-

ers have also been developed.[25–28] However, these theories were developed to describe the details of the step structures, including the terrace width distributions of each layer. Beyond two or three layers, they become very cumbersome and unrealistic. Recently, attempts[29,30] have been made to correlate the surface width of a finite layer system to the angular distribution of the diffraction intensity. It has been suggested that the surface width can be obtained by measuring the energy-dependent peak intensity or diffuse intensity at the vicinity of the central Bragg reflections near the in-phase condition in an electron-diffraction experiment. However, this model does not provide a method for measuring the generic scaling properties during growth, including the exponent α.

So far, the only diffraction theory capable of dealing with the growth problem is a continuous interface model proposed by Sinha *et al.*[31] Based on the assumption of the continuous surface structure, this model is designed to describe disordered systems such as amorphous solids and liquids. For a crystalline interface, it is only applicable in the case of "small-$k_\perp$" diffraction: $k_\perp c \ll \pi$, where c denotes the vertical lattice spacing and $k_\perp$ is the component of momentum transfer normal to the surface ($k = 2\pi/\lambda_0$, λ_0=diffraction wavelength). The discrete atomic structure of an interface can be safely ignored in small-$k_\perp$ diffraction experiments, using, for example, light scattering, neutron scattering, or grazing angle x-ray diffraction. However, as we pointed out previously,[32] a diffraction experiment performed at the small-$k_\perp$ condition is not sufficient for the study of dynamic scaling behavior during growth. As will be discussed in detail in this paper, some important scaling properties can only manifest themselves in the "larger-$k_\perp$" regime, $k_\perp c \sim \pi$, corresponding to the so-called out-of-phase diffraction condition. At the near out-of-phase condition, since the diffraction involves the destructive interference between different atomic layers in a surface, the discrete atomic structure of the interface cannot be ignored. Therefore, a full understanding of the dynamic growth phenomena from the point of view of diffraction requires necessarily an investigation starting from a generic discrete atomic structure with diffraction conditions covering both the in-phase and out-of-phase regimes.

In this paper, we will present a general approach to the aforementioned diffraction problem from stepped surfaces during growth for any value of $k_\perp c$. A Brief Report[32] focusing on the time-invariant behavior of dynamic growth has been published. In this paper, a detailed discussion has been devoted to both the time-dependent and time-invariant parts of the diffraction characteristics during growth in the different $k_\perp c$ regimes. Section II gives a brief description of the dynamic scaling features for both the height-height correlation function and the pair-correlation (height difference correlation) function. In Sec. III, diffraction from the growth front is discussed in detail. We first discuss general diffraction characteristics in the dynamic growth problem, and then focus on the details of the time-invariant and the time-dependent parts of the diffraction profiles, respectively. Section IV is a summary of this paper.

II. CORRELATION FUNCTIONS IN SURFACE GROWTH FRONT

A diffraction technique measures the surface correlation functions which statistically describe the surface morphology. Among these correlation functions, the most important ones are the height-height correlation function and the pair-correlation function (or the height difference correlation function).

A. Equal-time height-height correlation function

The equal-time height-height correlation function is defined as the mean square of the height difference measured simultaneously between two surface atomic positions separated by a lateral distance $\mathbf{r}$,

$$G(\mathbf{r},t)=\langle [h(\mathbf{r},t)-h(0,t)]^2\rangle, \tag{2}$$

where an atomic position in a surface is represented by $(\mathbf{r},z)$. The vertical coordinate (along the normal) $z=h(\mathbf{r},t)$ measures the surface atomic column height at the growth time t.

The dynamic scaling theory predicts that the surface morphology during growth undergoes both roughening and coarsening evolutions.[1–3] (We will not be concerned with the finite-size effect in this paper, because a realistic system should be sufficiently large, $L \gg t^{1/z}$.) Two correlation lengths along the vertical and lateral directions are assigned to describe the roughening and coarsening processes, respectively. The vertical correlation length is defined as the root-mean-surface height fluctuation $w(t)=\sqrt{\langle [h(\mathbf{r},t)-\langle h\rangle]^2\rangle}$, which measures the interface width shown in Eq. (1). The lateral correlation length $\xi(t)$, the distance over which surface fluctuations spread, characterizes the coarsening size at the growth time t. Similar to $w(t)$, $\xi(t)$ also evolves with time in a form of a power law, $\xi(t)\sim t^{1/z}=t^{\beta/\alpha}$.

Over a distance much larger than the lateral correlation length, the surface height fluctuations should not be correlated. The height-height correlation function, therefore, has a long-range asymptotic form

$$G(\mathbf{r},t)\sim 2[w(t)]^2 \quad (r \gg \xi). \tag{3}$$

Equation (3) follows from the identity,

$$\begin{aligned}\langle [h(\mathbf{r},t)-h(0,t)]^2\rangle = &\langle [h(\mathbf{r},t)-\langle h\rangle]^2\rangle \\ &+\langle [h(0,t)-\langle h\rangle]^2\rangle \\ &-2\langle [h(\mathbf{r},t)-\langle h\rangle] \\ &\times [h(0,t)-\langle h\rangle]\rangle,\end{aligned}$$

and $\langle [h(\mathbf{r},t)-\langle h\rangle]^2\rangle = \langle [h(0,t)-\langle h\rangle]^2\rangle = [w(t)]^2$.

On the other hand, the height-height correlation function has a short-range asymptotic form according to dynamic scaling,

$$G(\mathbf{r},t)\sim r^{2\alpha} \quad [r \ll \xi(t)\sim t^{1/z}]. \tag{4}$$

This is consistent with Eq. (1) if we set $L=r$.

The self-affine description of a growing interface, shown in Eq. (1), requires that any related correlation function has the form of the generalized homogeneous

function. For the height-height correlation function, this yields

$$G(\lambda \mathbf{r}, \lambda^{\alpha/\beta} t) = \lambda^{2\alpha} G(\mathbf{r}, t). \tag{5}$$

That is, if one rescales the surface by a factor of λ in the lateral direction, in order to observe the similarity between the original and the rescaled surface, one has to not only rescale the surface by a factor of λ^{α} in the vertical direction, but also rescale the time by a factor of $\lambda^{\alpha/\beta}$ corresponding to the time $t' = \lambda^{\alpha/\beta} t$.

In Eq. (5), let $\lambda = t^{-\beta/\alpha}$. One obtains a scaling equation,

$$G(\mathbf{r}, t) = t^{2\beta} G\left[\frac{\mathbf{r}}{t^{\beta/\alpha}}, 1\right]. \tag{6}$$

In order to be consistent with both the scaling relation, Eq. (6), and the asymptotic expressions, Eqs. (3) and (4), the equal-time height-height correlation function for a growing interface must have a form of

$$G(\mathbf{r}, t) = 2[w(t)]^2 g\left[\frac{r}{\xi(t)}\right], \tag{7a}$$

with the scaling function,

$$g\left[\frac{r}{\xi(t)}\right] \propto G\left[\frac{r}{t^{\beta/\alpha}}, 1\right]$$

given by

$$g(x) = \begin{cases} x^{2\alpha} & \text{for } x \ll 1 \\ 1 & \text{for } x \gg 1. \end{cases} \tag{7b}$$

A phenomenological scaling function, which has been used in the continuous surface model, was given by[31]

$$g(x) = 1 - e^{-x^{2\alpha}}. \tag{8}$$

Equation (7) addresses several important issues in a dynamic growth process.

(i) The scale-dependent surface roughness. The surface is rough on the short-range scale $r \ll \xi(t)$, but looks smooth on the long-range scale $r \gg \xi(t)$. The growing surface thus involves a large number of atomic layers but still has a finite interface width. The interface during growth is smoother than the equilibrium rough surface at $T \geq T_R$ but is rougher than the equilibrium flat surface at $T < T_R$, where T_R is the equilibrium roughening transition temperature.

(ii) The stationary state and the steady growth. On the short-range scale, Eq. (7) becomes

$$G(\mathbf{r}, t) \approx 2w^2 \left[\frac{r}{\xi}\right]^{2\alpha} = 2\left[\frac{r}{\eta}\right]^{2\alpha}, \tag{9}$$

where $\eta = \xi w^{-1/\alpha}$ is a time-invariant quantity, which in the case of a crystalline interface is interpreted as the average terrace size.[32] During the dynamic growth, the distributions of the local terraces and steps are stationary but the global surface roughness still evolves in time. This very interesting property, shown in Fig. 1(a), has been discussed in a previous publication.[32]

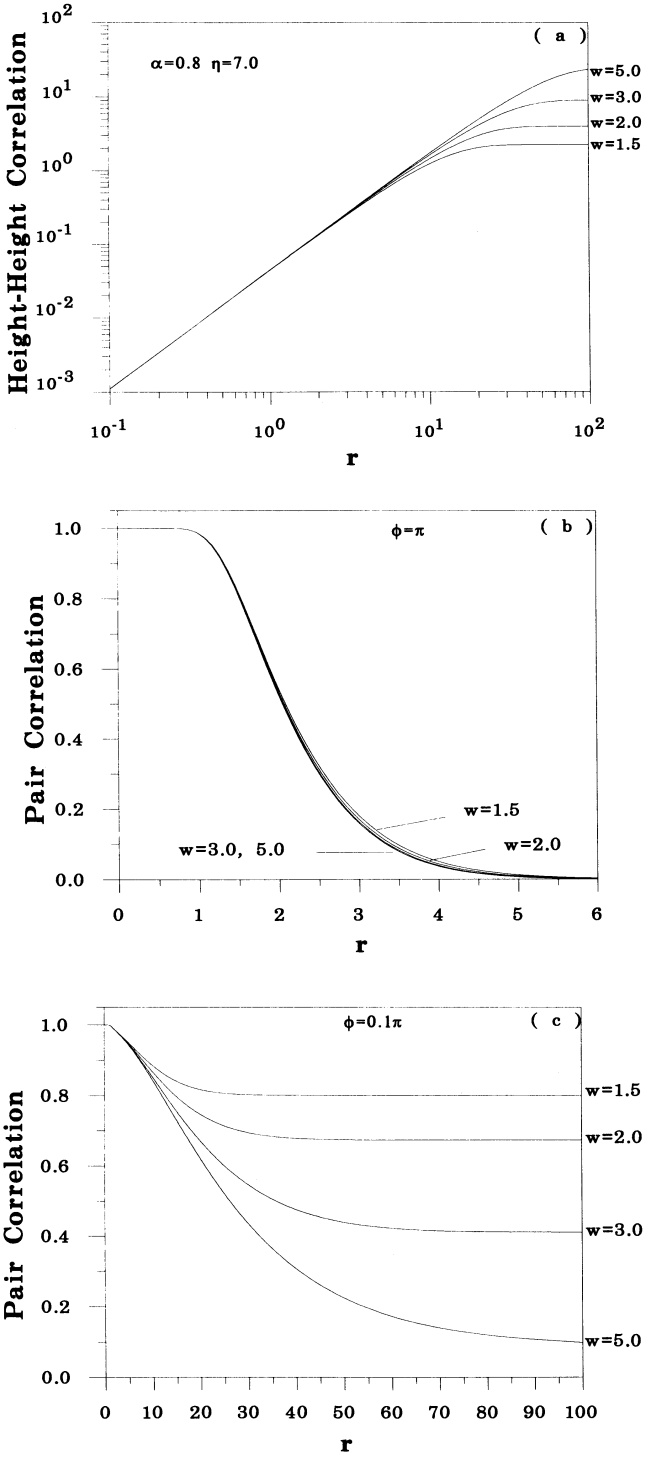

FIG. 1. Schematics of the surface correlation functions of a growing interface. (a) The equal-time height-height correlation function shown in Eq. (7), where the roughness exponent is $\alpha = 0.8$ and the average terrace size is $\eta = 7.0$ (in units of the lattice constant). The different values of w are the interface widths at different growth times. The relation between w and ξ is $\eta = \xi w^{-(1/\alpha)}$. Note that in the small-r regime, the correlation is time invariant. (b) and (c) The corresponding pair-correlation functions with discrete Gaussian approximation given by Eq. (12) at $\phi = \pi$ and $\phi = 0.1\pi$, respectively.

(iii) Fractal and the "discrete lattice effect." From Eqs. (4) and (7), a "$D=3-\alpha$" fractal[33] might be expected to exist in the local regime,[3,20] $r \ll r_c$, where r_c satisfies

$$\langle |h(r_c,t)-h(0,t)| \rangle \sim \sqrt{G(r_c,t)}=r_c,$$

i.e., $r_c \sim \eta^{-\alpha/(1-\alpha)}$. However, a crystalline surface, in general, is not a fractal on the atomic scale even though Eq. (5) demonstrates a self-affine behavior. In the absence of surface overhangs, the average domain size is $\eta > 1$ (in units of the lateral atomic spacing). The fractal regime $r \ll r_c < 1$ is seemingly cut off by the lattice constant because the scaling behavior, Eq. (5), does not exist within an atomic spacing. This discrete lattice effect has a significant impact on scaling behavior in the diffraction measurements, which will be discussed later.

B. Pair-correlation function (height difference correlation function)

Usually, in a diffraction experiment, one may not be able to directly measure the height-height correlation function. Instead, one can obtain the pair-correlation function through the Fourier transformation of the measured diffraction intensity. The diffraction structure factor $S(\mathbf{k}_\parallel, k_\perp, t)$, which is directly proportional to the diffraction intensity, represents the Fourier transform of the pair-correlation function,

$$S(\mathbf{k}_\parallel, k_\perp, t)=\int d^2r \exp(i\mathbf{k}_\parallel \cdot \mathbf{r}) \times \langle \exp\{ik_\perp c[h(\mathbf{r},t)-h(0,t)]\} \rangle, \quad (10)$$

where $\mathbf{k}_\parallel$ and $k_\perp$ are the wave vectors parallel and perpendicular to the surface, respectively. The pair-correlation function is defined as

$$C(\mathbf{r},\phi,t) \equiv \langle \exp\{i\phi[h(\mathbf{r},t)-h(0,t)]\} \rangle, \quad (11)$$

where the phase $\phi=k_\perp c$ determines the diffraction conditions. For $\phi=2n\pi$ ($n=0,\pm1,\pm2,\ldots$), constructive interference occurs in the diffraction, which corresponds to the in-phase diffraction conditions. In contrast, $\phi=(2n-1)\pi$ corresponds to the out-of-phase conditions at which the destructive interference dominates the diffraction. In order to calculate $C(\mathbf{r},\phi)$, one needs to know the statistical distribution function $\rho(\Delta h)$ for the relative surface height $\Delta h=h(\mathbf{r},t)-h(0,t)$, where $\rho(\Delta h)$ depends on the surface morphology. A simple approximation is to assume that $\rho(\Delta h)$ obeys a Gaussian distribution. In contrast to the continuous surface model where a continuous Gaussian distribution is assumed,[31] a discrete version of the Gaussian distribution function has to be used for a crystalline surface in which, $\Delta h=0,\pm1,\pm2,\ldots$ (in units of c). Using the discrete Gaussian approximations, Villain, Grempel, and Lapujoulade[23] have obtained an explicit form for the pair-correlation function which intrinsically connects to the height-height correlation of $G(\mathbf{r},t)$,

$$C(\mathbf{r},\phi,t) \approx \frac{\sum_{m=-\infty}^{m=+\infty} e^{-(1/2)G(\mathbf{r},t)(\phi-2\pi m)^2}}{\sum_{m=-\infty}^{m=+\infty} e^{-(1/2)G(\mathbf{r},t)(2\pi m)^2}}. \quad (12)$$

The important aspects of Eq. (12) are discussed as follows.

(i) Periodic oscillation. Due to the periodic and discrete structure of a crystalline surface, Eq. (12) gives the relations $C(\mathbf{r},\phi,t)=C(\mathbf{r},\phi+2n\pi,t)$ and $C(\mathbf{r},2n\pi,t)=1$. These are consistent with the definition, Eq. (11). Such relations cannot be obtained from the continuous surface model in which the pair correlation has been derived to give a form,[31]

$$C_c(\mathbf{r},\phi,t)=e^{-(1/2)\phi^2 G(\mathbf{r},t)}. \quad (13)$$

(ii) Lowest-order approximation. Equation (12) can be approximately represented by its lowest-order term,

$$C_0(\mathbf{r},\phi,t)=e^{-(1/2)[\phi]^2 G(\mathbf{r},t)}, \quad (14)$$

where $[\phi]$ means ϕ modulo 2π such that $-\pi \le [\phi] \le \pi$. At the small-$k_\perp$ diffraction condition $|\phi| \ll \pi$, Eq. (14) agrees with Eq. (13) for the continuous surface model. Equation (14) can hold for most cases but fails to provide a reasonable approximation at the near out-of-phase conditions. For comparison, we plot both $C_0(\mathbf{r},\phi,t)$ and $C(\mathbf{r},\phi,t)$ versus r in Fig. 2 at various phase conditions. The difference between $C_0(\mathbf{r},\phi,t)$ and $C(\mathbf{r},\phi,t)$ is negligibly small at the near in-phase condition, as shown in Fig. 2(a) where $\phi=0.1\pi$. At $\phi=0.5\pi$, shown in Fig. 2(b), the deviation $C_0(\mathbf{r},\phi,t)$ from $C(\mathbf{r},\phi,t)$ appears only in the small-r scale, but $C_0(\mathbf{r},\phi,t)$ is still a good approximation because the diffraction contribution from the small-r regime is much smaller than that from the larger-r regimes. However, at the out-of-phase condition ($\phi=\pi$), there are very significant deviations, as shown in Fig. 2(c). In fact, the difference between $C_0(\mathbf{r},\phi,t)$ and $C(\mathbf{r},\phi,t)$ results entirely from the discrete lattice effect. At the near in-phase conditions, which are similar to the small-$k_\perp$ cases, discrete lattice structure can be ignored, and likewise the deviation of $C_0(\mathbf{r},\phi,t)$ from $C(\mathbf{r},\phi,t)$. In contrast, at the near out-of-phase conditions, destructive interference from the discrete lattice comes into play so that $C_0(\mathbf{r},\phi,t)$, the lowest-order term, is not a good approximation to $C(\mathbf{r},\phi,t)$. For example, if $\phi \sim \pi$, both terms $e^{-(1/2)\phi^2 G(\mathbf{r},t)}$ and $e^{-(1/2)(2\pi-\phi)^2 G(\mathbf{r},t)}$ give the same contribution in Eq. (12). The approximation $C_0(\mathbf{r},\phi,t)$, which only contains the term $e^{-(1/2)\phi^2 G(\mathbf{r},t)}$, surely underestimates the value of $C(\mathbf{r},\phi,t)$.

(iii) Scaling features for different phase conditions. Dynamic scaling features are clearly shown in the evolution of the pair correlation $C(\mathbf{r},\phi,t)$ as a function of time. Figures 1(b) and 1(c) are plots of $C(\mathbf{r},\phi,t)$ for different values of $w(t)$. The former is for $\phi=\pi$, the out-of-phase diffraction condition and the latter for $\phi=0.1\pi$, the near in-phase condition. With the increase of $w(t)$ with time, shown in Fig. 1(b), $C(\mathbf{r},\phi=\pi,t)$ quickly converges into a unique and time-independent function. This function is confined in a short-range regime which corresponds to the time-invariant part of the height-height correlation [Fig. 1(a)]. In contrast, at the near in-phase condition shown in Fig. 1(c), $C(\mathbf{r},\phi=0.1\pi,t)$ shows a steady change with time and does not converge as in the out-of-phase case. Thus, the near in-phase pair correlation is most sensitive to the time-dependent global behavior of

the growing interface while the near out-of-phase pair correlation is most sensitive to the time-invariant local properties. Going from the in-phase to the out-of-phase conditions, the pair-correlation function exhibits different

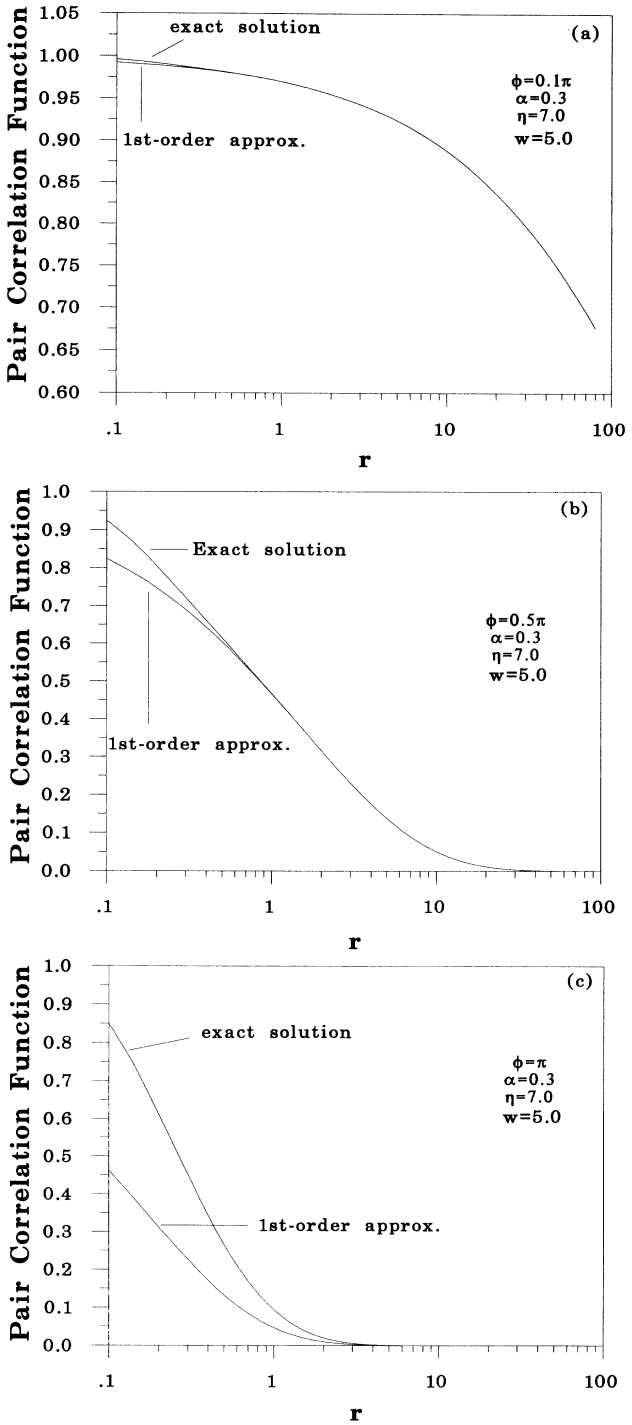

FIG. 2. Comparison between the rigorous pair-correlation function, Eq. (12), and its lowest-order approximation, Eq. (14), at various diffraction phase conditions: (a) $\phi=0.1\pi$, (b) $\phi=0.5\pi$, (c) $\phi=\pi$. See Sec. II B.

scaling features. This very important result allows one to separate the time-invariant part from the time-dependent part in a diffraction experiment, so that scaling properties can be readily measured and interpreted.

(iv) Scaling symmetry-breaking caused by the discrete lattice effect. As shown in case (iii) in Sec. II A, the self-affine scaling relation does not apply to the atomic-scale regime $r\sim 1$. This discrete lattice effect has a significant consequence on the pair-correlation function. In the continuous surface model, Eq. (13) is a self-affine scale-invariant function. From Eq. (5),

$$C_c(\lambda\mathbf{r},\lambda^{-\alpha}\phi,\lambda^{\alpha/\beta}t)=C_c(\mathbf{r},\phi,t).$$

Such a scale-invariant property for the pair correlation results from the fact that the structure factor given by Eq. (10) has to be a generalized homogeneous function scaled as

$$S(\lambda^{-1}\mathbf{k}_{\parallel},\lambda^{-\alpha}k_{\perp},\lambda^{\alpha/\beta}t)=\lambda^2 S(\mathbf{k}_{\parallel},k_{\perp},t).$$

However, from Eq. (12), the self-affine scale-invariant relation usually does not hold for a crystalline interface, i.e.,

$$C(\lambda\mathbf{r},\lambda^{-\alpha}\phi,\lambda^{\alpha/\beta}t)\neq C(\mathbf{r},\phi,t).$$

But for the small-$k_{\perp}$ diffraction condition, $C(\mathbf{r},\phi,t)\approx C_c(\mathbf{r},\phi,t)$ [see case (ii) in Sec. II B]. The self-affine scale-invariant relation can only exist in the small-$k_{\perp}$ regime which corresponds to a large scale in real space. On the contrary, for the large-$k_{\perp}$ regime which corresponds to a small scale in real space, the self-affine relation is destroyed by the atom-scale structure, as discussed in case (iii) in Sec. II A. It is the discrete lattice effect that leads to the failure of the self-affine scale-invariant description for the pair-correlation function. Such a symmetry-breaking effect reminds us that one has to be cautious when examining the dynamic scaling relations in a diffraction experiment.

III. DIFFRACTION STRUCTURE FACTOR FROM GROWTH FRONT

The diffraction structure factor, Eq. (10), can be calculated by utilizing the generic correlation function (12) combined with Eq. (7).

A. General properties of the diffraction structure factor

Equation (12) can be rewritten as $C(\mathbf{r},\phi,t)=A(\phi,t)+\Delta C(\mathbf{r},\phi,t)$ with

$$\begin{aligned} A(\phi,t)&=C(\mathbf{r}\to\infty,\phi,t)\ ,\\ \Delta C(\mathbf{r},\phi,t)&=C(\mathbf{r},\phi,t)-C(\mathbf{r}\to\infty,\phi,t).\end{aligned} \tag{15}$$

The diffraction structure factor, Eq. (14), turns out to be a sum of a central δ peak and a broad diffuse component,

$$S(\mathbf{k}_{\parallel},k_{\perp},t)=(2\pi)^2 A(\phi,t)\delta(\mathbf{k}_{\parallel})+S_{\rm diff}(\mathbf{k}_{\parallel},k_{\perp},t), \tag{16}$$

where the diffuse structure factor is

$$S_{\rm diff}(\mathbf{k}_{\parallel},k_{\perp},t)=\int d^2r\,\exp(i\mathbf{k}_{\parallel}\cdot\mathbf{r})\Delta C(\mathbf{r},\phi,t). \tag{17}$$

A further simplification occurs when the diffraction condition is not close to "out of phase" so that $C(\mathbf{r},\phi,t)$ can be replaced by its lowest-order term, Eq. (14) [see case (ii) of Sec. II B]. The approximation leads to

$$S(\mathbf{k}_\parallel,k_\perp,t)\approx(2\pi)^2 e^{-[\phi]^2[w(t)]^2}\delta(\mathbf{k}_\parallel)+S_{\rm diff}(\mathbf{k}_\parallel,k_\perp,t), \tag{18}$$

$$S_{\rm diff}(\mathbf{k}_\parallel,k_\perp,t)\approx 2\pi e^{-\Omega}\int_0^\infty r\,dr\{e^{\Omega[1-g(r/\xi)]}-1\}\times J_0(k_\parallel r)$$

$$=2\pi e^{-\Omega}\sum_{n=1}^{\infty}\frac{\Omega^n}{n!}\int_0^\infty r\,dr\left[1-g\left[\frac{r}{\xi}\right]\right]^n\times J_0(k_\parallel r), \tag{19}$$

where $J_0(x)$ denotes the zeroth-order Bessel function, Ω is given by $\Omega=[\phi]^2[w(t)]^2$, and it is a critical quantity for determining the scaling properties in a diffraction experiment. The last step in Eq. (19) is obtained by expanding $e^{\Omega[1-g(r/\xi)]}$ as a Taylor series.

Equations (16) and (18) show the correspondence between the line shape of a diffraction beam intensity and the surface morphology of a growing interface: a sharp central δ peak appears when the surface looks smooth on the long-range scale while a broad diffuse line shape shows up if the surface is rough on the short-range scale.

In Eq. (18), the amplitude of the δ peak is proportional to the Debye-Waller–like factor $e^{-[\phi]^2[w(t)]^2}$ which not only decays exponentially as $w(t)$ grows, but also oscillates between in-phase and out-of-phase diffraction conditions. Figures 3(a) and 3(b) show the plots of the exact expression $A(\phi,t)$ and its lowest-order approximation $e^{-[\phi]^2[w(t)]^2}$ at two interface widths, respectively, as the phase varied from in-phase to out-of-phase conditions. For comparison, we also plot in Fig. 3(c) the nonoscillatory Debye-Waller factor $e^{-\phi^2[w(t)]^2}$, corresponding to the case of the continuous surface model. The difference between $A(\phi,t)$ and $e^{-[\phi]^2[w(t)]^2}$ is significant at the near out-of-phase conditions, as shown Fig. 3(a) where $w(t)$ is small. However, such a difference can be ignored for a realistically larger interface width, because for $w(t)>1$, both $A(\phi,t)$ and $e^{-[\phi]^2[w(t)]^2}$ vanish quickly at $[\phi]\sim\pi$, as shown in Fig. 3(b). The vanishing of the δ intensity indicates that the diffraction line shape at the vicinity of the out-of-phase condition is purely diffusive as $w(t)>1$. In contrast to the case of a continuous surface [Fig. 3(c)], Figs. 3(a) and 3(b) exhibit an oscillatory behavior of the diffraction from a multilayer step surface: $A(\phi,t)$ and $e^{-[\phi]^2[w(t)]^2}$ reach the maximum (=1) at the in-phase conditions due to constructive interference, and then exponentially decay to minimum values at the out-of-phase conditions as a result of destructive interference of the diffraction from the multilayer step surface.

The form of the diffuse structure factor can be further understood from a simple example. Inserting Eq. (8) into Eq. (19), one has

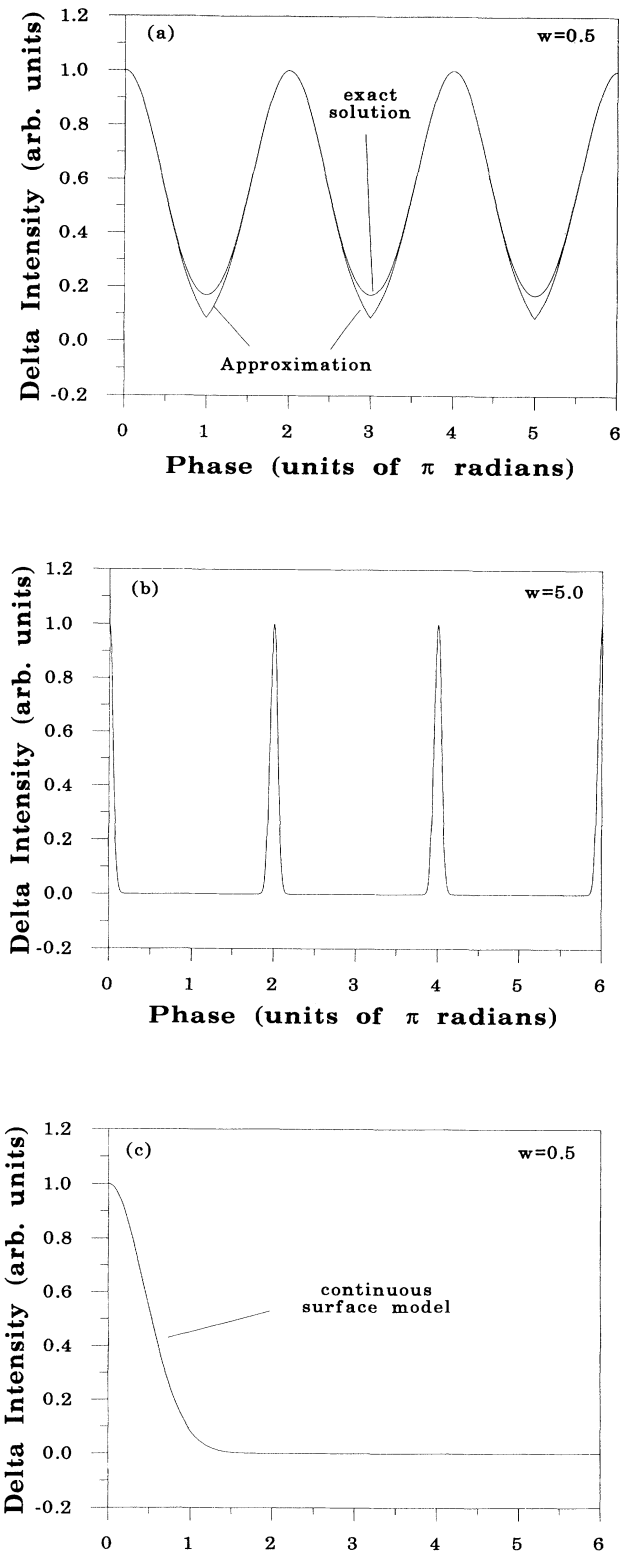

FIG. 3. The δ intensity of the diffraction line shape plotted as a function of the diffraction phase condition for (a) $w=0.5$, (b) $w=5.0$, and (c) the continuous surface model. Note that the δ intensity exhibits oscillatory behavior for a crystalline surface [(a) and (b)] but not in the case (c) of a continuous surface.

$$S_{\rm diff}(\mathbf{k}_\parallel,k_\perp,t)\approx 2\pi\xi^2 e^{-\Omega} \times \sum_{n=1}^{\infty}\frac{\Omega^n}{n!}\frac{1}{n^{1/\alpha}}F_\alpha(k_\parallel\xi n^{-1/2\alpha}), \quad (20)$$

where

$$F_\alpha(x)=\int_0^\infty y\,dy\,e^{-y^{2\alpha}}J_0(xy). \quad (21)$$

For $\alpha=0.5$, Eq. (20) turns out to be a sum of the two-dimensional (2D) Lorentzian functions,

$$F_{1/2}(k_\parallel\xi n^{-1})\propto\frac{1}{[1+(k_\parallel\xi n^{-1})^2]^{3/2}},$$

with different widths $\xi^{-1}n$, $n=1,2,\ldots$. A similar expression ($\alpha=0.5$) for the 1D ($d=1+1$) case has been obtained by Savage *et al.*[19] based on the continuous surface model,[31] where the function $F_{1/2}(k_\parallel\xi n^{-1})$ was replaced by the 1D Lorentzian function $1/[1+(k_\parallel\xi n^{-1})^2]$.

Interestingly, one may recall a similar situation in a model called the restricted Markovian chain, studied by Lent and Cohen.[25] This 1D Markovian surface is assumed to be confined within N atomic layers. The corresponding diffraction structure factor can be derived analytically as a central δ peak plus a diffuse profile which consists of 1D Lorentzians $1/[1+(k_\parallel/\omega_n)^2]$ with different widths ω_n. The number of the 1D Lorentzian components is $N-1$, as limited by the restricted atomic layers N.

In Eq. (20), the coefficient $(\Omega^n/n!)(1/n^{2\alpha})$ of the F_α function will quickly vanish as $n>\Omega=[\phi]^2[w(t)]^2$. The number of 2D Lorentzians which gives a significant contribution to the diffuse structure factor is actually limited by $w(t)$. Therefore, a growing surface with $d=2+1$ and $\alpha=0.5$ is suggested to be a "2D-restricted Markovian surface," and gives a diffuse structure factor consisting of 2D Lorentzian functions of a limited number determined by the interface width.

As we have pointed out in the last section, the general scaling relation in a diffraction measurement is broken by the discrete lattice effect. Only in the small-$k_\perp$ diffraction conditions where $|\phi|\ll\pi$ can Eqs. (17) and (19) show approximately a scaling relation

$$S(\lambda\mathbf{k}_\parallel,\lambda^\alpha k_\perp,\lambda^{-\alpha/\beta}t)\approx\lambda^2 S(\mathbf{k}_\parallel,k_\perp,t).$$

However, such a symmetry-breaking effect does not obstruct one from extracting the real-space dynamic scaling information in a diffraction experiment. The detailed methods, including the analysis of both time-invariant and time-dependent structure factors, will be presented next.

B. Time-invariant structure factor

The discussion starts from the lowest-order approximation, Eqs. (18) and (19), which can be calculated when a specific scaling function $g(x)$ is chosen. Given the phenomenological form of Eq. (8), Eq. (19) gives us Eq. (20) which, for the present purpose, can be rewritten as

$$S_{\rm diff}(\mathbf{k}_\parallel,k_\perp,t)\approx 2\pi\xi^2\int_0^\infty y\,dy\,e^{-y^{2\alpha}}\sum_{m=0}^{\infty}\frac{(-1)^m}{(m!)^2}\left[\frac{\mathbf{k}_\parallel\xi y}{2}\right]^{2m}\left[e^{-\Omega}\sum_{n=1}^{\infty}\frac{\Omega^n}{n!}n^{(1+m)/\alpha}\right], \quad (22)$$

where we expand the Bessel function

$$J_0(x)=\sum_{m=0}^{\infty}\frac{(-1)^m}{(m!)^2}\left[\frac{x}{2}\right]^{2m}.$$

For the case of $\Omega\gg1$, a useful asymptotic identity can be obtained (the rigorous proof is shown in the Appendix),

$$e^{-\Omega}\sum_{n=1}^{\infty}\frac{\Omega^n}{n!}n^{-(1+m)/\alpha}\approx\Omega^{-(1+m)/\alpha}\quad(\Omega\gg1).$$

Then, Eq. (22) simplifies to $S_{\rm diff}(\mathbf{k}_\parallel,k_\perp,t)\approx 2\pi([\phi]^{-1/\alpha}\eta)^2F_\alpha(k_\parallel|[\phi]|^{-1/\alpha}\eta)$, with $\eta=\xi w^{-(1/\alpha)}$. Also, for $[\phi]^2[w(t)]^2\gg1$, the δ peak in Eq. (18) is negligibly small, as shown in Fig. 3(b). Therefore, the diffraction structure factor becomes purely "diffusive" and time independent if $\Omega=[\phi]^2[w(t)]^2\gg1$,

$$S(\mathbf{k}_\parallel,k_\perp,t)\approx S_{\rm diff}(\mathbf{k}_\parallel,k_\perp,t)\approx 2\pi([\phi]^{-(1/\alpha)}\eta)^2F_\alpha(k_\parallel|[\phi]|^{-(1/\alpha)}\eta)\quad(\Omega\gg1). \quad (23)$$

Here α and η describe the time-invariant short-range behavior.

As shown in Fig. 1(a), the r-space height-height correlation is time invariant in the short-range regime $r\ll\xi(t)$. Accordingly, we have shown that the diffraction structure factor can also be time independent at certain $k_\perp$-space regimes. Such a time-invariant diffraction behavior occurs under the condition $\Omega\gg1$ at which the time-dependent central δ peak quickly drops to zero while the remaining diffuse component is purely a contribution from short-range scattering. This fact can also be understood from Fig. 1(b). One may define, in the reciprocal space of $k_\perp$, the time-invariant zones where the diffraction is dominated only by the short-range behavior as characterized by α and η. These zones are centered at the out-of-phase conditions $\phi-(2n-1)\pi$ with the ranges determined by the equation $\Omega=[\phi]^2[w(t)]^2\gg1$.

Although the above conclusions are obtained by introducing the phenomenological scaling function (8), it was shown rigorously in our earlier publication[32] that Eq. (23) is correct and "universal" for any form of $g(x)$ defined by Eq. (7b). The reason is simple: in the time-

invariant region, the diffraction structure factor can only detect the short-range behavior. For the short-range regime $x = r/\xi \ll 1$, the scaling function $g(x)$ has a universal form as shown in Eq. (9). The differences between different forms of $g(x)$ appear only in the longer distances $x > 1$ or $r > \xi$. For $\Omega \gg 1$, the diffraction is not sensitive at all to such a regime.

Equation (23) indicates that for $\Omega \gg 1$, the diffuse component shown in Eq. (20), which is a sum of the infinite number of F_α functions, has converged into a single F_α function with a different argument. A similar situation occurs in the case of the restricted 1D Markovian surface[25] corresponding to $d = 1+1$ and $\alpha = 0.5$, as discussed in Sec. III A. One recalls that a 1D random-step surface model, as studied by Lu and Lagally[22] (the LL model), involves an infinite number of atomic layers and leads to a diffraction structure factor containing only one Lorentzian function. This random-step model (LL model) is actually a special case of the restricted 1D Markovian chain studied by Lent and Cohen[25] (the LC model), with the number of the atomic layers $N \gg 1$. As the surface becomes rougher and rougher so that the number of the atomic layers N becomes significantly large, the diffuse structure factor which contains a large number $(= N-1)$ of 1D Lorentzians (LC model) will finally converge into a single 1D Lorenztian-type of function with a different width, as given by the LL model.

In the random-step surface model, the line shape of the structure factor has a full width at half maximum (FWHM) which oscillates between the in-phase and the out-of-phase conditions.[22] A similar oscillatory behavior can also be found from Eq. (23) for the FWHM as

$$2X_\alpha \frac{|[\phi]|^{1/\alpha}}{\eta} , \tag{24}$$

where the constant X_α satisfies $F_\alpha(X_\alpha) = 0.5F_\alpha(0)$. Furthermore, in the LL model, the FWHM is shown to be inversely proportional to the lateral average terrace size at the vicinity of $[\phi] \sim \pi$. The η in Eq. (24) should have a similar meaning and is proportional to the average terrace size at the growing surface.

So far, our specific structure factor calculation is based on the lowest-order approximation. Equations (18) and (19), however, do not apply to the vicinity of the out-of-phase conditions. The rigorous result, which does not have an analytical form, can be calculated numerically using Eqs. (16), (17), and (15). Figures 4(a) and 4(b) are plots of the diffraction structure factor using both rigorous and approximate calculations, respectively, at $[\phi] \sim 0.95\pi$ and at $[\phi] \sim 0.5\pi$. The deviation of the approximation from the rigorous calculation is significant at the near out-of-phase condition [Fig. 4(a)], but is negligibly small at $[\phi] \sim 0.5\pi$ [Fig. 4(b)]. The modification due to the discrete lattice effect can be seen in the plot of FWHM versus ϕ shown in Fig. 5. The cusp shape, which is predicted by Eq. (24) at $[\phi] \sim \pi$, actually becomes rounded according to the rigorous calculation. We must point out that such a modification due to the discrete lattice effect should not change the basic conclusions obtained so far. For example, if $\Omega \gg 1$, $A(\phi,t) = C(\mathbf{r} \to \infty, \phi, t) \to 0$, as shown in Eq. (16), which means that the diffraction structure factor becomes diffusive. The diffuse structure factor of Eq. (17) should be rigorously time invariant, because at $\Omega \gg 1$, it is only determined by the short-range height-height correlation, Eq. (9). Inserting Eq. (9) into Eq. (17), one can easily prove that at $\Omega \gg 1$, the general diffraction structure factor, Eq. (16), has a form

$$S(\mathbf{k}_\parallel, k_\perp, t) \approx S_{\text{diff}}(\mathbf{k}_\parallel, k_\perp, t) = H(k_\parallel \eta, \phi) \quad (\Omega \gg 1) ,$$

where $H(x,\phi)$ is a periodic function with respect to ϕ, $H(x,\phi) = H(x, \phi + 2\pi)$. Thus, the time-invariant parameter η can still be interpreted as the average terrace size because FWHM $\sim 1/\eta$.

Experimentally, the exponent α and the average terrace size η can be measured from the diffraction line shape as a function of the diffraction phase condition ϕ in the time-invariant zones. The step density can be obtained from the FWHM of the measured line shapes. As mentioned in our previous paper, if the approximate solu-

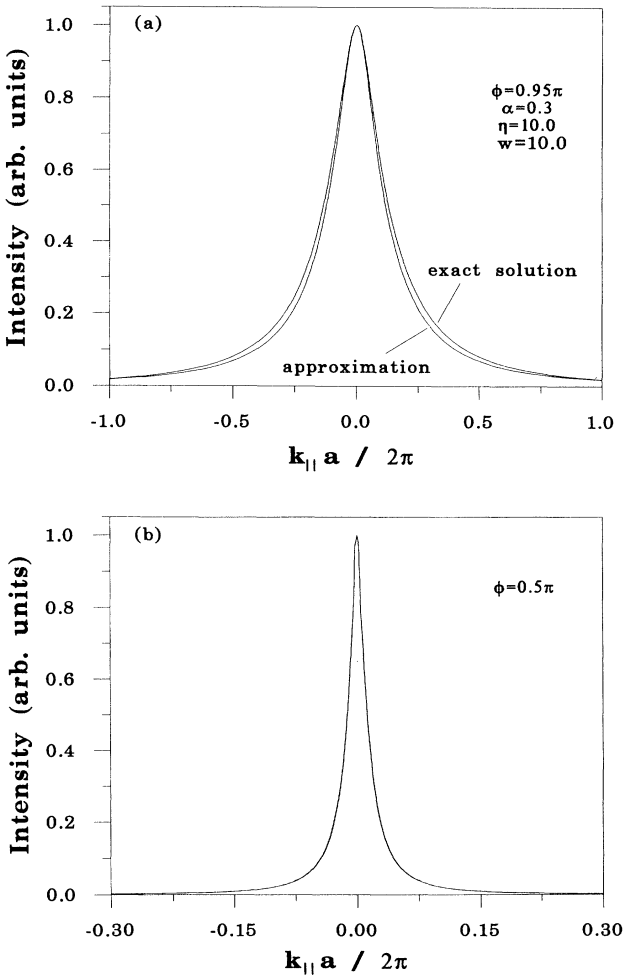

FIG. 4. Normalized line shapes of the diffraction structure factor using rigorous and approximate calculations. (a) Near out-of-phase condition $\phi = 0.95\pi$, (b) $\phi = 0.5\pi$. The difference between the two calculations is more significant in (a).

tion, Eq. (23), is used, the exponent α could be measured either from the log-log plot of intensity versus $|[\phi]|$ according to the power-law relation $S(0,k_\perp) \propto |[\phi]|^{-2/\alpha}$, shown in Eq. (23), or from the log-log plot of FWHM versus $[\phi]$ according to the power law $\text{FWHM} \propto |[\phi]|^{1/\alpha}$, from Eq. (24). We must emphasize that the methods of extracting α from the log-log plots may not be valid in a realistic situation because the discrete lattice effect always modifies the simple power-law relations described by Eqs. (23) and (24). As shown in Fig. 5, the modification due to the discrete lattice effect leads to the complete failure of the power-law description for $\alpha=0.8$ [Fig. 5(a)] while at $\alpha=0.3$, only in a small phase regime can such a power-law relation be preserved [Fig. 5(b)]. Therefore, a more reliable method should be based on the rigorous Eqs. (16), (17) and (15), and one can employ a numerical fitting method to analyze the experimental data. The rigorous relation of FWHM versus ϕ for several different values of α are plotted in Fig. 6, which can serve as standard curves for extracting the value of α.

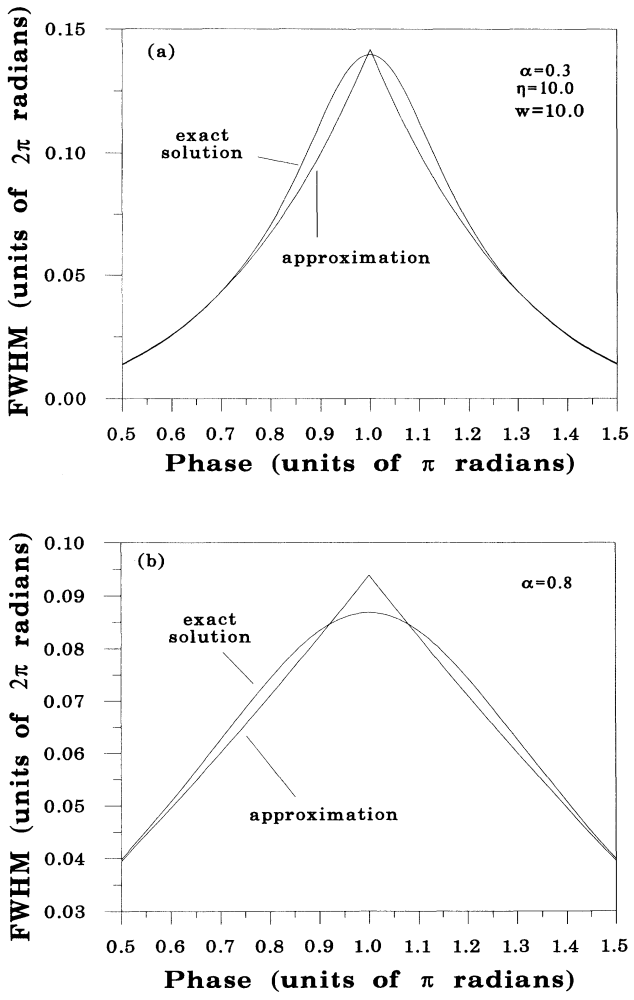

FIG. 5. Comparison of FWHM vs ϕ for rigorous and approximate calculations for (a) $\alpha=0.3$ and (b) $\alpha=0.8$.

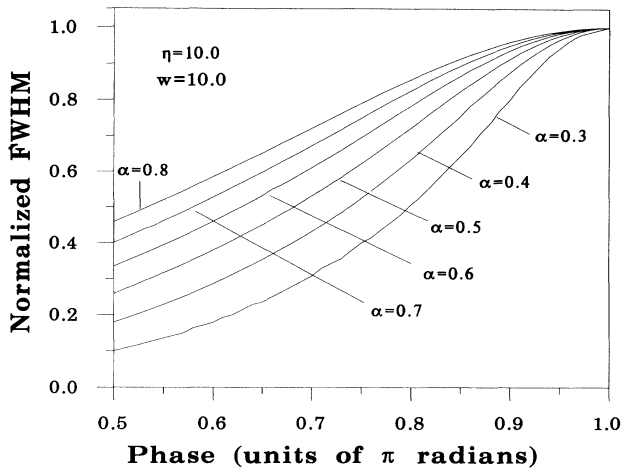

FIG. 6. Normalized FWHM vs diffraction phase ϕ for various values of the roughness exponents α at fixed η and w.

C. Time-dependent structure factor

In the regime $\Omega=[\phi]^2[w(t)]^2<1$, the diffraction structure factor is sensitive to the global (long-range) surface properties such as the time-dependent evolution of the growing interface. In contrast to the condition $\Omega \gg 1$, which defines the time-invariant zone with a diffraction structure factor only sensitive to the short-range behavior, the condition $\Omega \ll 1$ can define a time-dependent zone with a structure factor which is quite sensitive to the long-range behavior. The condition $\Omega=[\phi]^2[w(t)]^2 \ll 1$ is equivalent to the near in-phase diffraction condition $[\phi]\sim 0$, or $\phi \sim 2n\pi$, among which a simple case is the small-$k_\perp$ diffraction condition $\phi=k_\perp c \sim 0$. Diffraction at the near in-phase condition has been well studied by many authors, e.g., light scattering by Church, Jenkinson,and Zavada,[34] x-ray or neutron scattering by Sinha *et al.*[31] and by Savage *et al.*,[19] and LEED scattering by Henzler and co-workers.[29,30] These static diffraction results at small $k_\perp$ will serve as references in our present study of the interface growth problem.

Under the condition $\Omega \ll 1$, the diffraction structure factor can be further approximated as

$$S(\mathbf{k}_\parallel,k_\perp,t) \approx (2\pi)^2 e^{-\Omega}\delta(\mathbf{k}_\parallel) + 2\pi e^{-\Omega}\Omega\xi^2 \int_0^\infty x\,dx\,[1-g(x)]J_0(k_\parallel \xi x)\ , \tag{25a}$$

where the infinite order of summation in Eq. (19) is reduced to its first order with respect to Ω. The diffuse structure factor

$$S_{\text{diff}}(\mathbf{k}_\parallel,k_\perp,t) \approx 2\pi e^{-\Omega}\Omega\xi^2 \int_0^\infty x\,dx\,[1-g(x)]J_0(k_\parallel \xi x) \tag{25b}$$

depends on the specific form of the scaling function $g(x)$ in contrast to the case of the time-invariant zone.

Different scaling functions could behave differently in the crossover regime $x \sim 1$, i.e., $r \sim \xi(t)$, even though they have identical asymptotic forms in either short-range or long-range behavior as shown in Eq. (7b). If the phenomenological scaling functions, Eq. (8), is used, Eq. (25b) is simply proportional to a single F_α function,

$$S_{\text{diff}}(\mathbf{k}_\parallel, k_\perp, t) \approx 2\pi e^{-\Omega} \Omega \xi^2 F_\alpha(k_\parallel \xi) .$$

In fact, diffuse scattering at the near in-phase condition is much more sensitive to the crossover regime during growth. In contrast, in Eq. (25a), the δ-peak component is only sensitive to the long-range ($r \to \infty$) behavior and therefore is still independent of the form of $g(x)$. This component is given by

$$S_\delta(\mathbf{k}_\parallel, k_\perp, t) = (2\pi)^2 e^{-[\phi]^2[w(t)]^2} \delta(\mathbf{k}_\parallel) . \tag{25c}$$

Equation (25) also indicates that at the near in-phase condition, both the δ peak and the diffuse component are time dependent since they are functions of the interface width $w(t)$ and the lateral correlation length $\xi(t)$. $w(t)$ and $\xi(t)$, as well as the exponents α and $z = \alpha/\beta$, can be measured by the following methods.

(i) The δ-peak intensity at the near in-phase conditions. In contrast to the near out-of-phase conditions where the diffraction structure factor is purely diffusive, at the near in-phase conditions the diffuse intensity is quite weak and the δ peak becomes a predominant component. In Eq. (25c), the δ intensity is proportional to a Debye-Waller–like factor, $e^{-[\phi]^2 w^2}$, cf. the cases discussed by Wollschläger, Falta, and Henzler[30] and by Savage *et al.*[19] One can obtain the interface width $w(t)$ from the slope of the plot of the measured log-scale δ-peak intensity versus $[\phi]^2$,

$$\ln[S_\delta(\mathbf{k}_\parallel = 0, k_\perp, t)] \approx -[\phi]^2 w^2 + \text{ const} . \tag{26a}$$

Since $w(t) \propto t^{2\beta}$, one can also measure the exponent β from the time-dependent peak intensity during growth, $\ln[S_\delta(\mathbf{k}_\parallel = 0, k_\perp, t)] \propto -[\phi]^2 t^{2\beta}$, according to Eq. (26a).

(ii) Diffuse structure factor at the near in-phase conditions. From Eq. (25), the interface width $w(t)$ can also be obtained from the ratio of the integrated diffuse intensity to the integrated δ intensity,

$$\frac{\int d^2k_\parallel S_{\text{diff}}(\mathbf{k}_\parallel, k_\perp, t)}{\int d^2k_\parallel S_\delta(\mathbf{k}_\parallel, k_\perp, t)} = [\phi]^2 w^2 , \tag{26b}$$

where the integration of the δ peak is obtained from Eq. (25c),

$$\int d^2k_\parallel S_\delta(\mathbf{k}_\parallel, k_\perp, t) = (2\pi)^2 e^{-\Omega} \approx (2\pi)^2 \quad (\Omega \ll 1)$$

and the integration of the diffuse component, Eq. (17), is given by

$$\begin{aligned} \int d^2k_\parallel S_{\text{diff}}(\mathbf{k}_\parallel, k_\perp, t) &= \int d^2k_\parallel \int d^2r \exp(i\mathbf{k}_\parallel \cdot \mathbf{r}) \Delta C(\mathbf{r}, \phi, t) \\ &= (2\pi)^2 \Delta C(\mathbf{r} = 0, \phi, t) \approx (2\pi)^2 (1 - e^{-\Omega}) \approx (2\pi)^2 \Omega \quad (\Omega \ll 1) , \end{aligned}$$

where we have used the identity $\int d^2k_\parallel \exp(i\mathbf{k}_\parallel \cdot \mathbf{r}) = (2\pi)^2 \delta(\mathbf{r})$ and

$$\begin{aligned} \Delta C(\mathbf{r} = 0, \phi, t) &= C(\mathbf{r} = 0, \phi, t) - C(\mathbf{r} \to \infty, \phi, t) \\ &\approx 1 - e^{-\Omega} \quad \text{for } \Omega \ll 1 . \end{aligned}$$

The line shape of the diffuse structure factor, Eq. (25b), has a FWHM inversely proportional to the lateral correlation length,

$$\frac{2Yg}{\xi(t)} , \tag{26c}$$

where the constant Yg satisfies $H(Yg) = 0.5H(0)$, with the defined function, $H(y) = \int_0^\infty x\, dx\, [1 - g(x)] J_0(yx)$, which only depends on the scaling function $g(x)$. The lateral correlation length is thus experimentally measurable. Also because $\xi(t) \propto t^{1/z}$, one can measure the exponent z from the time-dependent FWHM during growth, i.e., FWHM $\propto t^{-1}/z$.

One may note that the FWHM does not vary with the phase ϕ at the near in-phase condition. This behavior is in contrast to that in the time-invariant zone where FWHM $\propto |[\phi]|^{1/\alpha}$, as shown in Eq. (24). Thus, the FWHM of the diffuse line shape is phase dependent and time independent at the near out-of-phase conditions, but is phase independent and time dependent at the near in-phase conditions.

(iii) Light scattering, LEED, and x-ray diffraction. Scattering of visible light uses a wavelength of the order of 10^3 Å. This means a phase condition of $\phi = k_\perp c \sim c/\lambda_0 \sim 10^{-3} \ll 1$ corresponds to a small-$k_\perp$ diffraction. In a light-scattering experiment, the angle-resolved optical scattering spectrum is given by[34]

$$\frac{1}{I_i} \left[\frac{dI}{d\Omega} \right]_s = 4k^4 \cos\theta_i \cos^2\theta_s R W(\mathbf{k}_\parallel) ,$$

where I's are the optical intensity and the θ's are the angles of the light beams with respect to the surface-normal direction. The subscripts i and s denote the incident and scattering directions, respectively. R is a quantity related to the optical reflectivity of a surface. In a angle-resolved optical scattering spectrum, the information of the surface roughness is contained in the optical power spectral density $W(\mathbf{k}_\parallel)$ defined as

$$W(\mathbf{k}_\parallel)=\frac{1}{A}\left\langle\left|\frac{1}{2\pi}\int d^2r\, e^{i\mathbf{k}_\parallel\cdot\mathbf{r}}h(\mathbf{r})\right|^2\right\rangle$$
$$=\frac{1}{A}\frac{1}{(2\pi)^2}\int d^2r\int d^2r' e^{i\mathbf{k}_\parallel\cdot(\mathbf{r}-\mathbf{r}')}\times\langle h(\mathbf{r})h(\mathbf{r}')\rangle$$
$$\propto\int d^2\rho\, e^{i\mathbf{k}_\parallel\cdot\rho}\langle h(\rho)h(0)\rangle\ ,$$

where A is the area illuminated by the incident light beam and the average height is chosen to be $\langle h(\mathbf{r})\rangle=0$. For the dynamic growth problem, the correlation function

$$\langle h(\mathbf{r})h(0)\rangle=w^2-\tfrac{1}{2}\langle[h(\mathbf{r})-h(0)]^2\rangle$$
$$=w^2\left[1-g\left[\frac{r}{\xi}\right]\right],$$

as shown in Eq. (7). The optical power spectral density turns out to be

$$W(\mathbf{k}_\parallel)\propto w^2\xi^2\int_0^\infty x\,dx\,[1-g(x)]J_0(k_\parallel\xi x)\ ,$$

which is proportional to the near in-phase diffuse structure factor given by Eq. (25b).

The comparison between light scattering and LEED has been discussed well by Pietsch, Henzler, and Hahn in an instructive way as shown in Fig. 1 of Ref. 29. Diffuse light scattering is more suitable for a rough surface which has a lateral correlation length comparable to the optical wavelength $\xi\sim\lambda_0\sim10^3$ Å. The light-scattering technique has a very narrow $k_\parallel$-space resolution, $|k_\parallel|\ll2\pi/\lambda_0\sim10^{-3}$ Å^{-1}. One can obtain the detailed fine structures of the diffuse line shape with FWHM$\sim1/\xi\sim10^{-3}$ Å^{-1} as $\xi\sim\lambda_0$, according to Eq. (26c). Neither x-ray nor LEED diffraction techniques can easily measure such a narrow diffuse profile even with their ultimate $k_\parallel$-space resolution, $|k_\parallel|\sim10^{-3}$ Å^{-1}. However, the light-scattering technique has a disadvantage that its adjustable range in the k space is very limited. Since $|k_\perp|_{\max}\le2\pi/\lambda_0\sim10^{-3}$ Å^{-1}, i.e., $\phi=k_\perp c\sim10^{-3}\ll1$, the time-invariant zone of a growing interface cannot be approached using this technique. Also, due to the very limited $k_\parallel$ space scanning range, $|k_\parallel|_{\max}\le2\pi/\lambda_0\sim10^{-3}$ Å^{-1}, light scattering is unable to measure the entire profile of a broader diffuse line shape if FWHM$>2\pi/\lambda_0$, corresponding to $\xi<\lambda_0$. Therefore, for a rough surface with its lateral correlation length shorter than the optical wavelength $\xi<\lambda_0$, the simple evaluation methods, as shown in case (ii) of Sec. III C are, in general, not valid for a diffuse light-scattering experiment. Of course, one can still evaluate the peak intensity of the diffuse line shape, which is proportional to $w^2\xi^2$ according to Eq. (25b), but the information is more involved since w and ξ cannot be easily separated. For situations such as these, it is more appropriate to use x-ray or LEED techniques which provide a much larger $k_\parallel$-space scanning range because $|k_\parallel|_{\max}\sim1$ Å^{-1}.

IV. SUMMARY

Starting from the general scaling hypothesis for the dynamic growth problem, we utilize a generic but stabilized (nondivergent) height-height correlation function to describe the growth front. The contribution of the discrete lattice effect is effectively included using the discrete Gaussian approximation. The diffraction intensity is calculated rigorously in the $d=2+1$ dimension. We show that the dynamic scaling behavior during growth can be examined by measuring the diffraction line shapes for in-phase and out-of-phase diffraction conditions. The predicted functional forms for the line shape, such as Eqs. (23) and (25), can be readily tested in a diffraction experiment. The growth exponents α and β which are relevant to the growth parameters can be deduced from the diffraction intensity in a number of different ways, either within one technique or with a combination of diffraction techniques. The results are expected to be very useful for experimental diffraction studies of the dynamic scaling behavior in complex nonequilibrium problems.

APPENDIX: PROOF OF THE ASYMPTOTIC EQUATION

We show

$$g(\Omega,\gamma)=e^{-\Omega}\sum_{n=1}^{\infty}\frac{\Omega^n}{n!}n^{-\gamma}\to\Omega^{-\gamma}\ \text{ as }\ \Omega\to\infty\ . \tag{A1}$$

The case of the integral γ was proved in our earlier publication.[32] This result can be extended to the nonintegral case.

$g(\Omega,\gamma)$ has a relation,

$$g(\Omega,\gamma)=e^{-\Omega}\Omega\sum_{n=1}^{\infty}\frac{\Omega^{n-1}}{n!}n^{-\gamma}$$
$$=e^{-\Omega}\Omega+e^{-\Omega}\Omega\sum_{n=1}^{\infty}\frac{\Omega^n}{n!}(n+1)^{-\gamma-1}\ . \tag{A2}$$

Using the identity,

$$\frac{1}{(n+1)^{\gamma+1}}=\frac{1}{n^{\gamma+1}(1+1/n)^{\gamma+1}}$$
$$=\sum_{k=0}^{\infty}\frac{\Gamma(-\gamma)}{\Gamma(-\gamma-k)}n^{-(k+\gamma+1)}\ , \tag{A3}$$

we reexpress Eq. (A2) as

$$g(\Omega,\gamma)=e^{-\Omega}\Omega+\Omega\sum_{k=0}^{\infty}\frac{\Gamma(-\gamma)}{\Gamma(-\gamma-k)}\times\left[e^{-\Omega}\sum_{n=1}^{\infty}\frac{\Omega^n}{n!}n^{-(k+\gamma+1)}\right]$$
$$=e^{-\Omega}\Omega+\Omega\sum_{k=0}^{\infty}\frac{\Gamma(-\gamma)}{\Gamma(-\gamma-k)}g(\Omega,k+\gamma+1)\ , \tag{A4}$$

where the last step is obtained using the definition of $g(\Omega,\gamma)$. If Ω tends to infinity, Eq. (A4) has a solution,

$$g(\Omega,\theta)=\frac{F(\Omega)}{\Omega^\theta}\ , \tag{A5}$$

where $F(\Omega)$ is the function of Ω and satisfies

$$\frac{e^{-\Omega}\Omega}{F(\Omega)\Omega^{-\gamma}} \to 0 \quad \text{as } \Omega \to \infty \ . \tag{A6}$$

To prove that (A5) is an asymptotic solution, we insert (A5) into the right-hand side (RHS) of Eq. (A4) and let $\Omega \to \infty$,

$$\text{RHS of Eq. (A4)} = e^{-\Omega}\Omega + \frac{F(\Omega)\Omega}{(1+\Omega)^{\gamma+1}} \to \frac{F(\Omega)}{\Omega^{\gamma}}$$
$$= g(\Omega,\gamma)$$
$$= \text{LHS of Eq.(A4)} ,$$

where we have used Eqs. (A3) and (A6). It is easy to determine the function $F(\Omega)$:

$$F(\Omega) = g(\Omega,0) = e^{-\Omega}\sum_{n=1}^{\infty}\frac{\Omega^n}{n!} = 1 - e^{-\Omega} \to 1 \quad \text{as } \Omega \to \infty \ .$$

Therefore, we have proven $G(\Omega,\gamma) = \Omega^{-\gamma}$.

[1]For reviews, see, F. Family, Physica A **168**, 561 (1990).

[2]Also see, *On Growth and Form,* edited by H. E. Stanley and N. Ostrowsky (Nijhoff, Boston, 1986).

[3]For a recent review, see, *Solids Far From Equilibrium: Growth Morphology and Defects,* edited by C. Godriche (Cambridge University Press, New York, 1991), pp. 432 and 479.

[4]S. F. Edwards and D. R. Wilkinson, Proc. R. Soc. London Ser. A **381**, 17 (1982).

[5]L. M. Sander, in *Multiple Scattering of Waves in Random Media and Random Rough Surfaces,* edited by V. V. Varadan and V. K. Varadan (Pennsylvania State University, University Park, PA, 1985).

[6]F. Family, J. Phys. A **19**, L441 (1986).

[7]R. Jullien and R. Botet, J. Phys. A **18**, 2279 (1985).

[8]J. G. Zabolitzky and D. Stauffer, Phys. Rev. A **34**, 1523 (1986); Phys. Rev. Lett. **57**, 1809 (1986).

[9]J. Kertész and D. E. Wolf, J. Phys. A **21**, 747 (1988); D. E. Wolf and J. Kertész, Europhys. Lett. **4**, 651 (1987).

[10]M. J. Vold, J. Colloid Sci. **14**, 168 (1959).

[11]F. Family and T. Vicsek, J. Phys. A **18**, L75 (1985).

[12]M. Kardar, G. Parisi, and Y. Zhang, Phys. Rev. Lett. **56**, 889 (1986).

[13]J. M. Kim and J. M. Kosterlitz, Phys. Rev. Lett. **62**, 2289 (1989).

[14]S. Das Sarma and P. Tamborenea, Phys. Rev. Lett. **66**, 325 (1991).

[15]Z.-W. Lai and S. Das Sarma, Phys. Rev. Lett. **66**, 2348 (1991).

[16]L.-H. Tang and T. Nattermann, Phys. Rev. Lett. **66**, 2899 (1991).

[17]Hong Yan, Phys. Rev. Lett. **68**, 3048 (1992).

[18]Elliott A. Eklund, R. Bruinsma, J. Rudnick, and R. Stanley Williams, Phys. Rev. Lett. **67**, 1759 (1991).

[19]D. E. Savage, J. Kleiner, N. Schimke, Y.-H. Phang, T. Jankowski, J. Jacobs, R. Kariotis, and M. G. Lagally, J. Appl. Phys. **69**, 1411 (1990).

[20]R. Chiarello, V. Panella, J. Krim, and C. Thompson, Phys. Rev. Lett. **67**, 3408 (1991), and references therein.

[21]M. A. Rubio, C. A. Edwards, A. Dougherty, and J. P. Gollub, Phys. Rev. Lett. **63**, 1685 (1989), and references therein.

[22]T.-M. Lu and M. G. Lagally, Surf. Sci. **120**, 47 (1982).

[23]J. Villain, D. R. Grempel, and J. Lapujoulade, J. Phys. F **15**, 809 (1985).

[24]M. den Nijs, E. K. Riedel, E. H. Conrad, and T. Engel, Phys. Rev. Lett. **55**, 1689 (1985).

[25]C. S. Lent and P. I. Cohen, Surf. Sci. **139**, 121 (1984).

[26]J. M. Pimbley and T.-M. Lu, J. Appl. Phys. **57**, 1121 (1985).

[27]M. G. Lagally, D. E. Savage, and M. C. Tringides, in *Reflection High-Energy Electron Diffraction and Reflection Electron Imageing of Surface,* edited by P. K. Larsen and P. J. Dobson (Plenum, New York, 1988), p. 139.

[28]M. Henzler, in *Reflection High-Energy Electron Diffraction and Reflection Electron Imageing of Surface,* edited by P. K. Larsen and P. J. Dobson (Plenum, New York, 1988), p. 193.

[29]G. J. Pietsch, M. Henzler, and P. O. Hahn, Appl. Surf. Sci. **39**, 457 (1989).

[30]J. Wollschläger, J. Falta, and M. Henzler, Appl. Phys. A **50**, 57 (1990).

[31]S. K. Sinha, E. B. Siroto, S. Garoff, and H. B. Stanley, Phys. Rev. B **38**, 2297 (1987).

[32]H.-N. Yang, T.-M. Lu, and G.-C. Wang, Phys. Rev. Lett. **68**, 2612 (1992).

[33]B. B. Mandelbrot, *The Fractal Geometry of Nature* (Freeman, New York, 1982).

[34]E. L. Church, H. A. Jenkinson, and J. M. Zavada, Opt. Eng. **16**, 360 (1977).